

Surface segregation behavior of B, Ga, and Sb during Si MBE: Calculations using a first-principles method

Jiro Ushio, Kiyokazu Nakagawa, Masanobu Miyao, and Takuya Maruizumi

Central Research Laboratory, Hitachi, Ltd., 1-280 Higashi-koigakubo, Kokubunji-shi, Tokyo 185, Japan

(Received 9 February 1998)

The potential energies of B, Ga, and Sb dopant atoms in the three top layers of Si(100) surfaces were evaluated using density-functional calculations of the model clusters. The different behaviors of the dopants in surface segregation during silicon molecular-beam epitaxy can be understood by considering the dopant-Si bond energies as the driving force for segregation. The energy of the B-Si bond is greater than that of the Si-Si bond, which precludes segregation, while the weaker Ga-Si and Sb-Si bonds favor it. [S0163-1829(98)06031-7]

I. INTRODUCTION

Silicon molecular-beam epitaxy (Si-MBE) has been developed to realize shallow and abrupt p - n junctions and heterostructures. However, recent experiments have shown that almost all dopant impurities (Al,¹ Ga,¹⁻³ and Sb³⁻⁵), except B,⁶ segregate to the surface during Si-MBE. This surface segregation lowers the doping efficiency and smears the doping profile.

Surface segregation during Si-MBE growth is essentially a dynamic process in which a dopant atom jumps from a subsurface to the surface. The behavior of the dopant can be explained by the two-state model^{7,8} based on the lower potential energy (the lower Gibbs free energy) of the dopant in the surface state than in the subsurface state. The dopant's jumping rate for surface segregation is determined by the potential barrier between the surface and subsurface states of the dopant, and the driving force of surface segregation is the energy difference between the two states. The dopant atom in the surface state is adsorbed on the Si surface. In the subsurface state, the dopant atom substitutes for a Si atom in the first surface Si layer; that is, the dopant atom is incorporated into the first Si layer, and a Si atom is adsorbed on the surface instead. This model provides a qualitative explanation of surface segregation behavior for Sn on GaAs (Ref. 7) and Sb on Si (Ref. 4) in a wide temperature range without any quantitative information on the potential energy curve. However, to understand the different segregation behaviors of dopants, and to find a way to control surface segregation, quantitative studies of the potential energy of dopants in crystals are indispensable.

We have evaluated the potential energies of B, Ga, and Sb atoms in Si(100) surface layers using accurate density-functional theory in the approximation of zero temperature. Accordingly, the obtained potential energy is not the Gibbs free energy, but the enthalpy, which is an important factor in surface segregation in alloys.⁹ We considered that the enthalpy as a function of the dopant's location in the Si crystal provides a sound basis for discussion of the behavior of the dopants in surface segregation during Si-MBE as well. Based on the calculated results, we investigate which is the primary

factor that controls surface segregation. We also discuss the Si lattice structures around the dopant atoms in the Si crystal.

II. COMPUTATIONAL DETAILS

We performed the calculations as follows. We first needed to determine the adsorption site of each of the B, Ga, and Sb atoms on the Si(100) surface. In the determination, we assumed the ideal Si(100) (1×1) surface as the surface on which a single dopant atom adsorbs, and we did not consider the interaction between the adsorbed dopants, for example, a dimer formation of the dopants on the surface. The four possible adsorption sites on a Si(100) surface are shown in Fig. 1(a). They are the bridge, hollow, antibridge, and on-top sites. To determine the most stable adsorption site, we calculated the total energies of Si clusters with dopant atoms at various heights from the surface. The structure of one of the Si clusters used here, Si₉H₁₂ which corresponds to a bridge site, is shown with a dopant atom in Fig. 1(b). The H atoms are used to terminate the dangling bonds of the Si atoms at the boundaries of the clusters. The nearest Si-Si and Si-H bond lengths were fixed to be 2.35 Å (taken from the Si crystal) and 1.48 Å (from SiH₄), respectively. The size of the clusters is large enough as a surface model to investigate the adsorption energies of a single dopant atom on the Si(100)

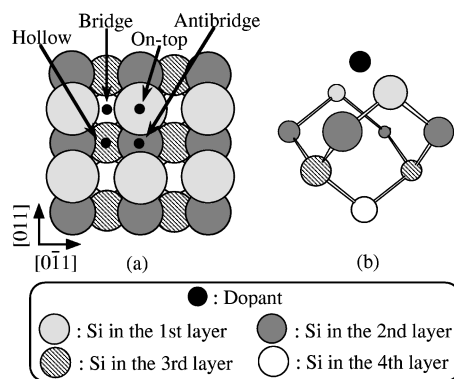


FIG. 1. (a) Possible adsorption sites on the Si(100) surface. (b) Cluster model for the bridge site adsorption (the dopant atom and Si₉H₁₂).

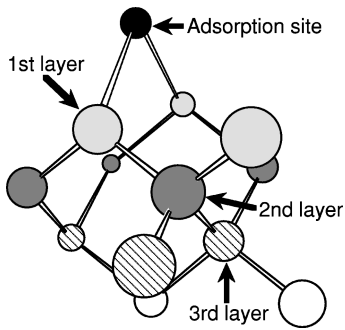


FIG. 2. Cluster model (the dopant atom and $\text{Si}_{12}\text{H}_{16}$) used to calculate the total energies of the cluster for the adsorbed and incorporated states of B, Ga, and Sb atoms on or in the Si(100) surface layers. The four locations where the dopant atom was placed to calculate the adsorbed and incorporated states are indicated by the arrows.

surface as Tang and Freeman reported,¹⁰ though a larger cluster is required to study the dimer formation of the adsorbed dopant atoms.

In order to calculate the three incorporated states of the dopant into the first to third Si surface layers with the same cluster model, we used a larger cluster, $\text{Si}_{12}\text{H}_{16}$. The structures of the incorporated states were generated by the exchange of an adsorbed dopant atom and a Si atom in the cluster. Figure 2 illustrates the cluster structure used here. Structural relaxation caused by the dopant incorporation was taken into account by searching for the most stable positions of the nearest Si atoms around the incorporated dopant atom using the analytical gradient method.¹¹

We performed all the calculations in the present study using the linear combination of Gaussian-type orbitals–model core potential–density-functional theory (LCGTO-MCP-DFT) program deMon.^{12–14} We considered explicitly all electrons for the B, Ga, Sb, and H¹⁵ atoms and valence electrons for the Si atom.¹⁶ The core electrons of the Si atom were replaced by the model core potential.¹⁶ The exchange-correlation functionals used were local ones developed by Vosko, Wilk, and Nusair.¹⁷ In our evaluation of the bond energies of the B-Si, Ga-Si, Sb-Si, and Si-Si bonds, we also used a gradient-corrected exchange functional developed by Perdew and Wang¹⁸ and a correlation functional developed by Perdew¹⁹ to obtain values more accurate than the local-density approximation and to confirm the validity of the order of the dopant-Si bond energies obtained from the local-density approximation. The respective electronic states of the Si cluster with and without a dopant atom were a closed shell having all electrons paired and an open shell having only one unpaired electron.

III. RESULTS AND DISCUSSION

A. Energetics of the adsorbed and incorporated states

The obtained adsorption energies for B, Ga, and Sb on the Si(100) surface are listed in Table I. The largest adsorption energies are 7.35 eV (the bridge site) for B, 4.56 eV (the hollow site) for Ga, and 5.28 eV (the hollow site) for Sb. The second largest adsorption energies are 5.25 eV (the hollow site), 4.32 eV (the bridge site), and 5.22 eV (the bridge site) for B, Ga, and Sb, respectively. The differences between the

TABLE I. Adsorption energies (E_{ad} in eV) and equilibrium heights from the surface (h in Å) of the B, Ga, and Sb atoms on the Si(100) surface.

Adsorption site	B		Ga		Sb	
	h	E_{ad}	h	E_{ad}	h	E_{ad}
Bridge	0.20	7.35	1.51	4.32	1.74	5.22
Hollow	-0.62	5.25	0.72	4.56	1.34	5.28
Antibridge	0.58	5.07	1.65	3.19	1.74	3.90
On-top	1.84	3.29	2.50	2.70	2.39	3.29

first and second largest adsorption energies for Ga and Sb are small, 0.24 eV for Ga and 0.06 eV for Sb. For simplicity, we neglected these small differences and assumed that the bridge site is the site that all the dopants in the adsorbed state occupy. If we adopted different adsorption sites for different dopants, we would have to use different Si clusters as models for the adsorbed and incorporated states of the dopants. This would cause a significant difference in the cluster-size effect on the potential-energy values for the different dopant atoms and would make it difficult to straightforwardly compare those potential energies. Use of a unique adsorption site and a unique Si cluster model for all the dopants enables us to eliminate such a problem.

The calculated total energies of the clusters as functions of the locations of the dopant atoms—that is, the potential energies for the dopant atoms—are shown in Fig. 3. The location of a dopant atom is denoted by the layer number of the layer where the dopant atom is located. As can be seen, the energies of the B-incorporated states where the B atom occupies one of the incorporation sites in the cluster, are lower than that of the B-adsorbed state where the B atom occupies the adsorption site on the cluster surface. On the other hand, all of the energies of the incorporated states of Ga and Sb are higher than those of the adsorbed states. The incorporated-state energies for both Ga and Sb increase monotonically as they go deeper from the adsorption site to the third Si layers. These calculated results offer a clear explanation for the experimental observations that B does not segregate to the Si surface during Si-MBE, but Ga and Sb do.

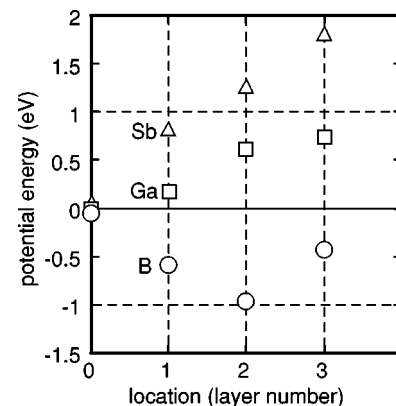


FIG. 3. Total energies of the Si cluster with dopant atoms of B, Ga, and Sb in the three surface layers of the Si(100) surface. The adsorbed state energy was taken as zero. The actual locations of the dopant atoms are shown by the arrows in Fig. 2.

TABLE II. Bond energies (in eV) of the B-Si, Ga-Si, Sb-Si, and Si-Si single bonds and their bond lengths (in Å) for the B, Ga, and Sb atoms in the second and third layers.

Bond	Bond energy ^a	Bond length ^b	
		Second layer	Third layer
B-Si	4.32 (3.75)	2.01	2.08
Ga-Si	3.42 (3.01)	2.32	2.36
Sb-Si	3.11 (2.53)	2.56	2.51
Si-Si	3.73 (3.30)	2.36 ^c	2.36 ^c

^aCalculated for the bonds in $\text{H}_2\text{B-SiH}_3$, $\text{H}_2\text{Ga-SiH}_3$, $\text{H}_2\text{Sb-SiH}_3$, and $\text{H}_3\text{Si-SiH}_3$ using the local exchange-correlation potential developed by Vosko, Wilk, and Nusair. The values in the parentheses were obtained from the gradient-corrected exchange-correlation potentials developed by Perdew and Wang.

^bFor B and Ga, the values are averages of the three bond lengths between the dopant and nearest-neighbor Si atoms. For Sb, the values are averages of the four Sb-nearest-neighbor Si bond lengths.

^cAverage of the four bond lengths between the Si atom in the third layer and the nearest-neighbor Si atoms in the optimized structure of the $\text{Si}_{12}\text{H}_{16}$ cluster without a dopant atom.

Here, we discuss the origin of the difference in the total energies. When the dopant incorporation takes place, dissociation and formation of the dopant-Si and Si-Si bonds occur. The energy balance due to the dissociation and formation of these bonds determines the stability of the incorporated state. We can crudely account for the energy balance by simply counting the number of bonds in the incorporated and adsorbed states. A group-III dopant atom, in spite of its valency, can make a fourth bond with a Si atom, but such a bond should be weaker than the other three dopant-Si bonds. The group-III element atom in the incorporated state can only make less-than-optimum dopant-Si bonds with the Si atoms in the Si crystal, compared with the three optimum bonds that can be formed with Si atoms that move freely. As a result, the group-III element atom in an incorporated state can be better stabilized by interaction with the fourth Si atom in the nearest neighbors. We assumed that all the Si-Si bonds (in the Si bulk and at the surface) have equal bond energies irrespective of the bonding types, such as in the Si bulk and as at the Si surface. As shown in Fig. 2, the incorporated dopant atoms in the first and second layers have three and four nearest-neighbor Si atoms, respectively. As the dopant atom goes from the adsorption sites in the first and second layers, the number of dopant-Si bonds increases by one (from 2 to 3) in the first layer and by two (from 2 to 4) in the second layer, while the number of Si-Si bonds of the entire cluster decreases by one in the first layer and by two in the second layer. Therefore, if the bond energy of the dopant-Si bond is larger than that of the Si-Si bond, the incorporated states in the first and second layers should be more stable than in the adsorbed state.

In the second column of Table II, we summarized the single-bond energies of the B-Si, Ga-Si, Sb-Si, and Si-Si bonds. These were obtained from calculations for $\text{H}_2\text{B-SiH}_3$, $\text{H}_2\text{Ga-SiH}_3$, $\text{H}_2\text{Sb-SiH}_3$, and $\text{H}_3\text{Si-SiH}_3$, respectively. The bond energy of B-Si is larger than that of Si-Si, but those of the Ga-Si and of Sb-Si bonds are smaller. Hence, from the

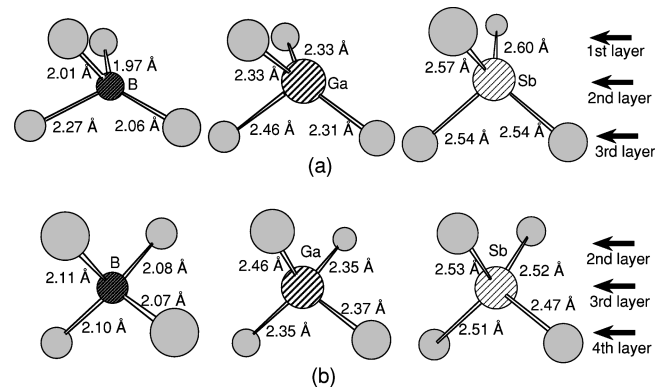


FIG. 4. Optimized structures around the dopant atoms in (a) the second layer, and (b) the third layer of the Si(100) surface.

discussion above, we would expect the potential energy of a B atom to decrease as the B atom goes from the adsorption site down to the incorporation site in the second layer and the potential energies of Ga and Sb to increase with their depth. This expectation agrees well with the results in Fig. 3. In particular, the potential energies of the dopants in the first layer correspond well to the differences between the dopant-Si and the Si-Si bond energies listed in Table II. We can conclude that the difference between the B-Si and Ga-Si bond energies is the primary cause of the completely different behaviors of B and Ga in surface segregation.

The incorporated state energy of B in the third layer is higher than in the first and second layers. This is because of a structural factor that destabilizes the dopant atom in the third or a deeper layer. The same factor also raises the potential energies of Ga and Sb in the third and deeper layers. In the next section, we give a detailed analysis of the structures of the incorporated states to explain this destabilization mechanism.

B. Structures of the incorporated states

We will analyze the structures of the incorporated states of the dopants to see the cause of the stability difference between the incorporated states of each dopant atom in the different layers. For this purpose, we compare the structures of the incorporated states of the dopant atoms in the second and third layers. Though there are four dopant-Si bonds in both the second and third layers, the potential energies of all the dopant atoms rise when moving from the second to the third layer. This energy rise must be caused by a difference in the structures of the incorporated states. Figure 4 shows the structures around the B, Ga, and Sb atoms in the incorporated states in the second and third surface layers. From Fig. 4(a), it can be seen that three B-Si or Ga-Si bonds are located almost on a plane that includes the three nearest-neighbor Si atoms (two in the first layer and one in the third layer). Consequently these three bonds among the four dopant-surrounding Si bonds are shorter than the remaining one. The averages of the three shorter-bond lengths are 2.01 Å and 2.32 Å for B and Ga, respectively (see Table II). Thus the group-III dopants in the second layer are almost planarly threefold coordinated.

The structures around the group-III dopant atoms in the third layer have a more tetrahedral nature, as shown in Fig.

4(b), and should have higher energies than in the second layer. The three shorter bonds between the group-III dopant atom and three nearest-neighbor Si atoms are slightly longer than those in the second layer. As a result, the differences in the bond lengths of the four dopant-Si (nearest-neighbor) bonds are smaller compared with those for the dopant atoms in the second layer. The average of the three shorter dopant-Si bonds for each dopant in the third Si layer is listed in the fourth column of Table II. For B and Ga, the average is larger than that in the second layer, by 0.07 Å for B and 0.04 Å for Ga. These findings all imply that the structures around the dopant atoms in the third layer are closer to those of the bulk Si crystal.

As for the Sb atom in the second layer, the structure around it is close to a tetrahedral coordination with four Sb-Si bonds of almost equal length. The average of those bond lengths is 2.56 Å. The average of the Sb-Si bond lengths for the Sb atom in the third layer is smaller by 0.05 Å than that in the second layer in contrast to the elongation of the B-Si and Ga-Si bonds that occurs when the B and Ga atoms go from the second layer to the third layer, as mentioned above. The averages of all the dopant-Si bond lengths in the second layer for B, Ga, and Sb are summarized in the third column of Table II. These correspond well to the bond lengths obtained from sums of the atomic covalent radii of dopant and Si atoms. The covalent radii are 0.81 Å for B, 1.25 Å for Ga, 1.41 Å for Sb, and 1.17 Å for Si.

Considering these results, we conclude that the energy rise for the incorporated state of a dopant atom as its depth increases from the second to a deeper layer (Fig. 3) is due to the increased rigidity of the Si network around the dopant atom. Energetically most favorable structures, such as those in the second layer shown in Fig. 4(a), cannot be realized in a deeper layer. Only the strained structures described in Fig. 4(b) are allowed there. For the incorporated states of a dopant atom in a much deeper (fourth or deeper) layer, we anticipate that the potential energy will change little from that in the third layer and that the structure around the dopant atom will also be similar to that in the third layer.

Note that the high level of stability of the incorporated state of B is not due to the smaller size of the B atom compared with a Si atom. An incorporated B atom distorts the surrounding Si lattice more than a Ga atom as shown in Fig. 4 and Table II. For the incorporated state in the second layer, the B-Si bond length of 2.01 Å differs by as much as 0.34 Å from the Si-Si bond length in the Si crystal, 2.36 Å, calculated for the Si atom in the third layer of the Si cluster without any adsorbed dopant atom on the surface. On the other hand, the Ga-Si bond length, 2.36 Å, is equal to the Si-Si bond length. The nearest-neighbor Si atoms around the B atom are located far from their positions in the pure Si crystal, and the Si atoms around the Ga atom remain almost at their original position. This greater distortion of the Si lattice due to the B incorporation, compared to that of the Ga incorporation, should destabilize the Si lattice more. However, the B incorporation actually stabilizes the system by as much as 0.58 eV, while the Ga incorporation causes destabilization of 0.18 eV (Fig. 3). This result implies that the atomic sizes of the B and Ga dopants do not affect the stability of their incorporated states, but the bond energies do. Consequently,

we conclude that the driving force of surface segregation of B, Ga, and Sb is primarily the dopant-Si bond energies, not their atomic sizes.

We should note that the potential barrier between the surface and subsurface states is important to understand the dynamic behavior of the dopant, the dominant factor of the surface segregation. However, in the present calculations the barrier height has not yet been obtained, because its evaluation would require a great deal of computer processing time. We obtained a higher potential energy of Sb than that of Ga, which means a larger driving force for the segregation of Sb than that of Ga. This seems to contradict the larger incorporation coefficient of Sb than Ga observed in a previous Si-MBE experiment.³ This may be due to the difference in the barrier heights for Sb and Ga.

IV. SUMMARY

The driving force of surface segregation of B, Ga, and Sb dopant atoms on a Si(100) surface was investigated with a theoretical approach using accurate density-functional theory. The different behaviors of the dopants in surface segregation can be understood by comparing the bond energies of the dopant-Si and Si-Si bonds. When a dopant atom goes from an adsorption site on the Si surface to an incorporation site in the surface Si layer, the number of dopant-Si bonds increases and the number of Si-Si bonds decreases. The incorporated state of the dopant atom is more stable than the adsorbed state if the energy gain due to the increased number of dopant-Si bonds surpasses the energy loss caused by the decreased number of Si-Si bonds. Consequently, a dopant atom that makes a bond with a Si atom that is stronger than the Si-Si bond can make the incorporated state more stable than the adsorbed state and can preclude surface segregation. A similar conclusion has been reported for surface segregation for alloys of the form $A_xB_{1-x}C$ by Patrick *et al.*⁹ Based on this consideration and the bond energies of B-Si, Ga-Si, and Sb-Si bonds, the differences in the calculated potential energies and the experimental observations for B, Ga, and Sb can be explained.

The incorporated state of B is most stable in the second layer because of the energy balance between the stabilization due to the bond formation between the B atom and the nearest-neighbor Si atoms and the destabilization due to the rigidity of the Si lattice around the B atom.

Although the incorporation of the B atom into the Si crystal causes a larger distortion of the surrounding Si lattice than is caused by the incorporation of the Ga atom, which is also a group-III element, the incorporated state of B is more stable than the adsorbed state, while the incorporated state of Ga is less stable than the adsorbed state. This suggests that the bond energy between the dopant and Si atoms is the dominant factor in surface segregation and that the atomic size of the dopant is less important in controlling the segregation.

ACKNOWLEDGMENT

We thank Yoshiaki Takemura of CRL, Hitachi, Ltd. for his help in the optimization of the structure for the adsorbed states of B.

- ¹G. E. Becker and J. C. Bean, *J. Appl. Phys.* **48**, 3395 (1977).
- ²T. Sakamoto and H. Kawanami, *Surf. Sci.* **111**, 177 (1981).
- ³K. Nakagawa, M. Miyao, and Y. Shiraki, *Thin Solid Films* **183**, 315 (1989).
- ⁴J. C. Bean, *Appl. Phys. Lett.* **33**, 654 (1978).
- ⁵H. Jorke, *Surf. Sci.* **193**, 569 (1988).
- ⁶N. L. Matthey, M. Hopkinson, R. F. Houghton, M. G. Dowsett, D. S. McPhail, T. E. Whall, E. H. C. Parker, G. R. Booker, and J. Whitehurst, *Thin Solid Films* **184**, 15 (1990).
- ⁷S. Hofmann and J. Erlewein, *Surf. Sci.* **77**, 591 (1978).
- ⁸J. J. Harris, E. E. Ashenford, C. T. Foxon, P. J. Dobson, and B. A. Joyce, *Appl. Phys. A: Solids Surf.* **33**, 87 (1984).
- ⁹R. S. Patrick, A.-B. Chen, A. Sher, and M. A. Berding, *Phys. Rev. B* **39**, 5980 (1989).
- ¹⁰S. Tang and A. J. Freeman, *Phys. Rev. B* **48**, 8068 (1993).
- ¹¹R. Fournier, J. Andzelm, and D. R. Salahub, *J. Chem. Phys.* **90**, 6371 (1989).
- ¹²A. St-Amant and D. R. Salahub, *Chem. Phys. Lett.* **169**, 387 (1990).
- ¹³A. St-Amant, Ph.D. thesis, Université de Montréal, 1991.
- ¹⁴D. R. Salahub, R. Fournier, P. Mlynarski, I. Papai, A. St-Amant, and J. Ushio, in *Density Functional Methods in Chemistry*, edited by J. Labanowski and J. Andzelm (Springer, New York, 1991), p. 77.
- ¹⁵N. Godbout, J. Andzelm, D. R. Salahub, and E. Wimmer, *Can. J. Chem.* **70**, 560 (1992).
- ¹⁶J. Andzelm, E. Radzio, and D. R. Salahub, *J. Chem. Phys.* **83**, 4573 (1985).
- ¹⁷S. H. Vosko, L. Wilk, and M. Nusair, *Can. J. Phys.* **58**, 1200 (1980).
- ¹⁸J. P. Perdew and Y. Wang, *Phys. Rev. B* **33**, 8800 (1986).
- ¹⁹J. P. Perdew, *Phys. Rev. B* **33**, 8822 (1986); **34**, 7406 (1986).